Noname manuscript No.
(will be inserted by the editor)

A two-stage stochastic PDE-constrained optimization approach to vibration control of an electrically conductive composite plate subjected to mechanical and electromagnetic loads

D. Chernikov · P. Krokhmal · O. I. Zhupanska · C. L. Pasiliao

Received: date / Accepted: date

Abstract A new two-stage stochastic partial differential equation (PDE)-constrained optimization methodology is developed for the active vibration control of structures in the presence of uncertainties in mechanical loads. The methodology relies on the two-stage stochastic optimization formulation with an embedded first-order black-box PDE-constrained optimization procedure. The PDE-constrained optimization procedure utilizes a first-order active-set algorithm with a conjugate gradient method. The objective function is determined through solution of the governing PDEs and its gradient is computed using automatic differentiation with hyper-dual numbers. The developed optimization methodology is applied to the problem of post-impact vibration control (via applied electromagnetic field) of an electrically conductive carbon fiber reinforced composite plate subjected to an uncertain, or stochastic, impact load. The corresponding governing PDEs consist of a nonlinear coupled system of equations of motion and Maxwell's equations. The conducted computational study shows that the obtained two-stage optimization solution allows for a significant suppression of vibrations caused by the randomized impact load in all impact load scenarios. Also, the effectiveness of the developed methodology is illustrated in the case of a deterministic impact load, where the two-stage strategy enables one to practically eliminate post-impact vibrations.

Keywords PDE-constrained optimization · two-stage stochastic optimization · electro-magneto-mechanical coupling · composite materials

Dmitry Chernikov
Department of Mechanical and Industrial Engineering
University of Iowa, Iowa City, IA 52241
E-mail: dmitry-chernikov@uiowa.edu

Pavlo Krokhmal
Department of Mechanical and Industrial Engineering
University of Iowa, Iowa City, IA 52241
Tel.: +1-319-335-5680
Fax: +1-319-335-5669
E-mail: krokhmal@engineering.uiowa.edu

Olesya I. Zhupanska
Department of Mechanical and Industrial Engineering
University of Iowa, Iowa City, IA 52241
E-mail: ozhupans@engineering.uiowa.edu

Crystal L. Pasiliao
Air Force Research Lab, Eglin AFB, FL 32542
E-mail: crystal.pasiliao@eglin.af.mil

1 Introduction

In electrically conductive solids, mechanical and electromagnetic fields interact through the Lorentz ponderomotive force that is exerted by the electromagnetic field. Analysis of this field interaction requires simultaneous solution of Maxwell's equations for electromagnetic field (Maugin, 1988) and equations of motion of continuous media that involve the Lorentz force as a body force, whereby the system of governing equations becomes coupled and nonlinear. This field coupling leads to many interesting effects observed in the mechanical behavior of the electrically conductive solids subjected to electromagnetic load, including changes in the stress state (Moon, 1984; Zhupanska and Sierakowski, 2007, 2011; Higuchi et al, 2007), vibration behavior (Barakati and Zhupanska, 2012a; Rudnicki, 2002), and unusual stability behavior (Hasanyan and Piliposyan, 2001; Hasanyan et al, 2006; Eringen, 1989).

Electro-magneto-mechanical field coupling represents a fundamental physical phenomenon that can potentially be employed for development of *multifunctional* or *adaptive* structures, i.e. structures capable of performing multiple functions and/or adapting their performance with respect to changes in the operating environment. In this context, the present work considers the issue of *active control* of structure's mechanical response by the electromagnetic field.

Composite materials are often considered to be materials of choice for multifunctional applications (Gibson, 2010) due to their multiphase nature and inherent tailorability. As a result, the recent years witnessed a growing interest in electro-magneto-mechanical interactions in composites. Most of the studies have been focused on the mechanics, while less attention was paid to the optimization of multifunctional composites and structures. The present work makes contribution to the latter subject.

The present work is closely related to the recent studies on the electro-magneto-mechanical coupling in electrically conductive anisotropic composites (Zhupanska and Sierakowski, 2007, 2011; Barakati and Zhupanska, 2012a,b, 2013, 2014), where the effects of the steady, slowly varying, and pulsed electromagnetic fields on the mechanical response of single-layer and laminated anisotropic composite plates were examined. The interacting effects of the applied electric current, external magnetic field, and mechanical load were studied. It has been shown that the characteristics of the electromagnetic field (waveform, duration of application, intensity) can significantly reduce the stressed and deformed states of the electrically conductive plate and decrease the amplitude of vibrations. In particular, to achieve the maximum reduction in the plate deflection and stress, the application of the mechanical load must be coordinated with application of the electric current and its waveform. Moreover, an increase in the magnetic induction tends to reduce the amplitude of vibrations of the plate with a trend towards a more rapid decay at the stronger magnetic fields. An increase in the electric current density tends to decrease the amplitude of the plate vibrations. Furthermore, the effect of the electric current density becomes more pronounced as the magnetic field intensity increases. It has been concluded that concurrent application of a pulsed electromagnetic load could effectively mitigate the effects of the impact load and post-impact vibrations.

1.1 Active vibration control of a composite plate via an electromagnetic field: A conceptual application

The results of the discussed above studies provided motivation for the present work on a stochastic partial differential equation (PDE)-constrained optimization approach to active control of the mechanical response of the electrically conductive composites, using an electromagnetic field. As a specific application, we consider the problem of vibration control – via application of an electromagnetic field – in an electrically conductive carbon fiber reinforced polymer (CFRP) composite plate subjected to a mechanical impact load with uncertain parameters (magnitude, duration, etc). We hypothesize that electromagnetically activated CFRP structural elements could provide additional protection against certain types of foreign object impacts, assuming that an appropriate sensor technology can be employed for applying an electromagnetic field to the composite structure at the moment of impact so as to increase the impact resistance and dampen post-impact vibrations.

The practical viability of this hypothetical scenario depends on a number of factors, among which are the availability of (i) composite materials with necessary mechanical and electromagnetic properties, (ii) adequate sensors to trigger application of an electromagnetic field, and (iii) ability to adjust and control characteristics of the applied electromagnetic field (i.e., waveform, duration of application, intensity) depending on the target composite material characteristics and applied impact load. Physics-based models of electro-magneto-mechanical coupling in electrically conductive composites can provide theoretical underpinnings for the development of the electromagnetically activated impact resistant structural elements, while PDE-constrained stochastic optimization can provide a path to the active control of these structural elements in the presence of uncertainties.

In Section 2.1 we outline the physical model of the field coupling phenomenon that is exploited in this work. Since the general model is prohibitively complex, a high-fidelity approximation of the governing equations in the case of thin composite plates is discussed. In Section 2.2 we introduce the dynamic nonlinear boundary-value problem corresponding to the impact of a thin CFRP composite plate in a deterministic setting, i.e. when the impact load is known with certainty. This problem forms the basis for the two-stage stochastic PDE-constrained optimization problem that is introduced in Section 3. Numerical solution and optimization procedures are discussed in Section 4, and in Section 5 we present the results of computational studies.

The authors view this work's contribution to literature in presenting a framework for dynamic adaptive control of the mechanical response of structures to randomized loads that is facilitated through the methods of two-stage stochastic optimization. The feasibility and effectiveness of the approach are illustrated on a dynamic nonlinear problem of impact of a CFRP plate, where the dynamic two-stage control action is implemented using the phenomenon of electro-magneto-mechanical field coupling in composites.

Among the studies that relate to the presented problem and proposed approach most closely, we may mention PDE-constrained optimization under dynamic loads considered by Min et al (1999), where the homogenization design method was used to find an optimal topology of a structure so as to minimize the dynamic compliance during a specified time interval. Kang et al (2001) proposed a method for dynamic design optimization that substitutes dynamic loads with equivalent sets of static loads that have similar effects and are updated at critical times. Zhang and Kang (2014) studied the control of a dynamic response of a thin-shell

structure, where sensing and actuation was done by using piezoelectric materials, and the goal was to find the optimal actuator/sensor layout, minimizing the vibration level over a specified time interval.

Shape optimization with randomized loads was considered in Conti et al (2009), where it was formulated in the form of a two-stage stochastic optimization problem. An important difference of the adaptive two-stage stochastic framework that is proposed in this work with that of Conti et al (2009) is that the latter is rather a clever mathematical device that frames a non-adaptive shape selection procedure in a two-stage form (see Section 3.2 for details).

2 Mechanics of electro-magneto-mechanical interactions in electrically conductive anisotropic composite plates

In this section we first outline the governing equations for anisotropic electrically conductive solids subjected to mechanical and electromagnetic loads. Then, we discuss a 2D plate approximation, as well as the resulting 2D nonlinear hyperbolic-parabolic system of PDEs that constitute the mathematical framework for solving problems of the dynamic mechanical response of the anisotropic electrically conductive plates subjected to mechanical and electromagnetic loads. See Zhupanska and Sierakowski (2007); Barakati and Zhupanska (2012a) for details.

2.1 Governing equations

The behavior and interaction of the mechanical and electromagnetic fields in electrically conductive solids can be determined from simultaneously solving the equations of motion that include the Lorentz ponderomotive force and Maxwell's equations:

$$\boldsymbol{\nabla}\cdot\mathbf{T}+\rho(\mathbf{F}+\mathbf{F}^{L})=\rho\frac{\partial^{2}\mathbf{u}}{\partial t^{2}}, \tag{1}$$

$$\begin{aligned}&\operatorname{div}\mathbf{D}=\rho_{e}, \qquad \operatorname{div}\mathbf{B}=0,\\ &\operatorname{rot}\mathbf{E}=-\frac{\partial\mathbf{B}}{\partial t}, \quad \operatorname{rot}\mathbf{H}=\mathbf{j}+\frac{\partial\mathbf{D}}{\partial t}.\end{aligned} \tag{2}$$

Here $\mathbf{T}$ is the stress tensor, $\mathbf{u}$ is the displacement vector, ρ is density, $\mathbf{F}$ is the body force per unit mass, $\mathbf{F}^{L}$ is the Lorentz force per unit mass, and ∇ is the gradient operator. In Maxwell's equations (2), $\mathbf{D}$ represents the electric displacement vector, $\mathbf{B}$ is the magnetic induction, $\mathbf{E}$ is the electric field, $\mathbf{H}$ is the magnetic field, $\mathbf{j}$ is the current density vector, ρ_e is the electric charge density (which vanishes in electric conductors), and t is time.

Interaction between mechanical and electromagnetic fields in the electrically conductive materials is due to the Lorentz force, $\mathbf{F}^{L}$, that enters equations of motion (1) as a body force. It has been shown in Zhupanska and Sierakowski (2007) that the Lorentz force in the electrically conductive anisotropic solids takes the form:

$$\begin{aligned}\rho\mathbf{F}^{L}=&\rho_{e}\left(\mathbf{E}+\frac{\partial\mathbf{u}}{\partial t}\times\mathbf{B}\right)+\left(\boldsymbol{\sigma}\left(\mathbf{E}+\frac{\partial\mathbf{u}}{\partial t}\times\mathbf{B}\right)\right)\times\mathbf{B}\\&+\left(\left((\boldsymbol{\varepsilon}-\varepsilon_{0}\mathbf{I})\,\mathbf{E}\right)\times\mathbf{B}\right)_{\alpha}\nabla\left(\frac{\partial\mathbf{u}}{\partial t}\right)_{\alpha}+\mathbf{J}^{*}\times\mathbf{B},\end{aligned} \tag{3}$$

where $\boldsymbol{\sigma}$ is the electrical conductivity tensor, $\boldsymbol{\varepsilon}$ is the electrical permittivity tensor, ε_0 is the electrical permittivity in the vacuum, ∇ is the gradient operator, and Einstein's summation convention is adopted with respect to index α. Therefore, the system of equations (1)–(2) is the system of nonlinear hyperbolic PDEs that represent the governing equations of electro-magneto-mechanical coupling in electrically conductive solids. The nonlinearity is due to the presence of the Lorentz force, which contains nonlinear terms with respect to the components of the mechanical and electromagnetic fields. In the most general dynamic case, the problem of solving the system of governing equations (1)–(2) for solids of even the simplest 3D geometries is insurmountable. In many situations, however, solution of equations (1)–(2) can be facilitated through appropriate *physics-based hypotheses*, or simplifications that allow one to reduce mathematical complexity of the model while preserving its physical fidelity by exploiting particular features of problem's geometry, etc.

With respect to the present work, a 2D approximation for the thin electrically conductive plates subjected to mechanical and electromagnetic loads is used. This approximation was developed in Zhupanska and Sierakowski (2007) and utilizes Kirchhoff hypothesis of non-deformable normals and electromagnetic hypotheses.

Next, we briefly outline the procedure to derive 2D approximation of the governing equations. More details can be found in Zhupanska and Sierakowski (2007); Barakati and Zhupanska (2012a). As for the mechanical part of the governing equations (1), the linear plate theory formulation based on the so-called Kirchhoff hypothesis of nondeformable normals is used. Equations of motion with respect to stress and moment resultants are obtained by integration of (1) across the thickness of the plate. In contrast to the problems with purely mechanical load, application of the Kirchhoff hypothesis and integration of the 3D equations of motion through the thickness of the plate does not produce 2D equations of motion. This is due to the presence of the terms with the Lorentz force components, which remain three-dimensional. Therefore, to obtain a 2D approximation to the equations of motion, one needs to derive a 2D approximation for the electromagnetic field and the Lorentz force for the case of thin plates. This is achieved by introducing additional hypotheses regarding the behavior of the

electromagnetic field components, which imply that tangential components of the electric field vector and the normal component of the magnetic field vector do not change across the thickness of the plate and the variation of the tangential components of the magnetic field across the thickness of the plate is linear. A 2D approximation of Maxwell's equations (2) is obtained by representing functions **H**, **E**, and **J** via series expansions with respect to the coordinate z, integrating Maxwell's 3D equations across the thickness of the plate and invoking a quasistatic approximation for Maxwell's equations. The 2D expression for the Lorentz force is obtained (3) using the Kirchhoff hypothesis for the plate displacements and the set of the discussed electromagnetic hypotheses. The 2D equations of motion are then obtained by integrating the terms with the Lorentz force across the thickness of the plate in the equations of motion with respect to the stress and moment resultants.

Finally, 2D equations of motion and 2D Maxwell's equations constitute the system of governing equations for a mechanically and electrically conductive plate subjected to mechanical and electromagnetic loads and correspond to the linear plate theory. This system of equations is a nonlinear mixed system of parabolic and hyperbolic PDEs.

2.2 Impact problem: A deterministic formulation

In this section we present the boundary-value problem for a thin anisotropic composite plate subject to a deterministic mechanical impact load and electromagnetic field within the mathematical framework presented in the previous subsection. Such a deterministic formulation was considered in Barakati and Zhupanska (2012a) and forms the basis for the stochastic model with uncertain impact loads and the corresponding stochastic optimization formulations will be introduced in Section 3.

Consider a thin unidirectional fiber-reinforced (x-direction is the fiber direction) electrically conductive composite plate of width a and thickness h subjected to the transverse impact load:

$$\mathbf{p}(x,y,t) = \big[0,0,p_z(x,y,t)\big], \tag{4}$$

time-dependent electric current of density:

$$\mathbf{J}(t) = \big[J_x(t),0,0\big], \tag{5}$$

and immersed in the constant magnetic field with the induction:

$$\mathbf{B}^* = \big[0,B_y^*,0\big]. \tag{6}$$

It is assumed that the intensity of the current is such that the associated thermal effects are negligible.

The plate is transversely isotropic, where y–z is the plane of isotropy and the x–y plane coincides with the middle plane of the plate. The plate is assumed to be long in the fiber direction, which is also the direction of the applied current (x-direction), simply supported along the long sides, arbitrarily supported along the short sides (see Figure 1), and initially is at rest.

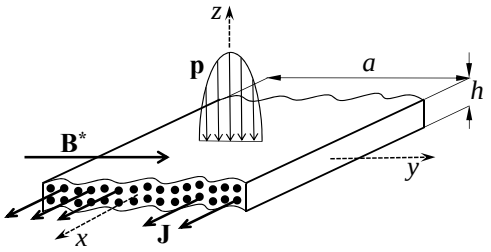

Fig. 1 Composite plate subjected to impact and electromagnetic loads

The corresponding mechanical and electromagnetic boundary conditions are:

$$\tau_{zz}\big|_{z=\frac{h}{2}} = -p_z(y,t), \tag{7a}$$

$$u_y\big|_{y=\pm\frac{a}{2}} = u_z\big|_{y=\pm\frac{a}{2}} = M_{yy}\big|_{y=\pm\frac{a}{2}} = 0, \tag{7b}$$

$$\Big(E_x - \frac{\partial w}{\partial t}B_y^* + \frac{\partial v}{\partial t}B_z\Big)\Big|_{y=-\frac{a}{2}} = 0, \quad E_x\Big|_{y=\frac{a}{2}} = 0. \tag{7c}$$

The applied transverse impact load (4) causes vibrations in the plate, which can potentially be mitigated by application of the external electromagnetic field consisting of the electric current of density (5) and magnetic induction (6). We are interested in the optimal characteristics of the electromagnetic field to maximally reduce mechanical vibrations caused by the impact load.

The formulated problem (4)-(7) for a long transversely isotropic plate admits the assumption of independence of the components of mechanical and electromagnetic fields of the coordinate x, which using the procedure described in Section 2 reduces the governing equations (1) and (2) to the form:

$$\begin{aligned}
\frac{1}{h}\frac{\partial N_{yy}}{\partial y} &= \rho\frac{\partial^2 v}{\partial t^2} + \sigma_x B_z^2\frac{\partial v}{\partial t} - \sigma_x B_y^* B_z\frac{\partial w}{\partial t} + \frac{\varepsilon_x-\varepsilon_0}{B_{22}}E_x B_z \\
&\quad\times\frac{\partial N_{yy}}{\partial t} - (\varepsilon_x-\varepsilon_0)E_x B_y^*\frac{\partial W}{\partial t} + B_z J_x(t) + \sigma_x E_x B_z, \\
\frac{1}{h}\frac{\partial N_{yz}}{\partial y} &= \rho\frac{\partial^2 w}{\partial t^2} + \frac{p_z(y,t)}{h} - \sigma_x B_y^* B_z\frac{\partial v}{\partial t} + \sigma_x\left(B_y^*\right)^2\frac{\partial w}{\partial t} \\
&\quad - (\varepsilon_x-\varepsilon_0)E_x B_z\frac{\partial W}{\partial t} - B_y^* J_x(t) - \sigma_x E_x B_y^*, \\
\frac{\partial M_{yy}}{\partial y} &= -\frac{\rho h^3}{12}\frac{\partial^2 W}{\partial t^2} + N_{yz} - \frac{1}{12}\sigma_x h^3 B_z^2\frac{\partial W}{\partial t} \\
&\quad + \frac{\varepsilon_x-\varepsilon_0}{B_{22}}E_x B_z\frac{\partial M_{yy}}{\partial t}, \\
\frac{\partial v}{\partial y} &= \frac{1}{hB_{22}}N_{yy}, \quad \frac{\partial^2 w}{\partial y^2} = -\frac{12}{h^3 B_{22}}M_{yy}, \quad \frac{\partial w}{\partial y} = W,
\end{aligned} \tag{8}$$

$$\frac{\partial B_z}{\partial y} = \sigma_x \mu \left(E_x + \frac{\partial v}{\partial t} B_z - \frac{\partial w}{\partial t} B_y^* \right), \quad \frac{\partial E_x}{\partial y} = \frac{\partial B_z}{\partial t}.$$

Here v and w are the middle plane displacement components in y- and z-directions, respectively; $N_{yy} = \int_{-h/2}^{h/2} \tau_{yy} dz$ and $N_{yz} = \int_{-h/2}^{h/2} \tau_{yz} dz$ are the stress resultants; $M_{yy} = \int_{-h/2}^{h/2} \tau_{yy} z dz$ is the moment resultant; E_x is the x-component of the electric field; B_z is the z-component of the magnetic induction; σ_x and ε_x are the electrical conductivity and permittivity in x-direction, respectively; μ is the magnetic permeability; and $B_{22} = E_2/(1-\nu_{12}\nu_{21})$, where E_2 is Young's modulus along the y-direction, ν_{12}, and ν_{21} are the corresponding Poisson ratios.

The system of the nonlinear PDEs (8) represents the governing equations in the context of this work. The formulated deterministic boundary-value problem (7)–(8) for low-velocity impact of a thin composite plate in the presence of an electromagnetic field forms the basis for the stochastic PDE-constrained optimization model of optimal vibration mitigation that is presented in Section 3.

3 A two-stage stochastic PDE-constrained optimization framework

In this section we first introduce a deterministic PDE-constrained optimization problem for vibration reduction in composite plates using an electromagnetic field, which is followed by the more general two-stage stochastic PDE-constrained optimization framework for control of composite structures in the presence of uncertainties in mechanical loads.

3.1 A PDE-constrained optimization formulation

The existence of field coupling effects between mechanical and electromagnetic fields in electrically conductive solids presents an opportunity for controlling and/or optimizing the mechanical response of the corresponding structures via application of an electromagnetic field. Assuming that the design or performance criterion of the structural element can be expressed through some function F to be minimized, the problem of optimization or control of the mechanical field via electromagnetic field generally reduces to a (nonlinear) PDE-constrained optimization problem of the form:

$$\min_{\boldsymbol{\theta}} \quad F_{[0,T]}(\mathbf{g}, \boldsymbol{\theta}, \boldsymbol{\xi}) \tag{9a}$$

$$\text{s. t.} \quad \frac{\partial \mathbf{g}}{\partial y} = \boldsymbol{\Phi}\left(\mathbf{g}, \frac{\partial \mathbf{g}}{\partial t}, \frac{\partial^2 \mathbf{g}}{\partial t^2}, \boldsymbol{\theta}, \boldsymbol{\xi} \right), \quad t \in [0,T], \tag{9b}$$

$$\mathbf{G}\left(\mathbf{g}, \frac{\partial \mathbf{g}}{\partial t} \right)\Big|_{y=\pm\frac{a}{2}} = \mathbf{0}, \quad t \in [0,T], \tag{9c}$$

$$\underline{\boldsymbol{\theta}} \le \boldsymbol{\theta} \le \overline{\boldsymbol{\theta}}, \tag{9d}$$

where vector $\mathbf{g}$ represents the components of the mechanical field, i.e., displacements and stress and moment resultants in the governing equations (8), vector $\boldsymbol{\theta}$ contains the parameters of the electromagnetic field (which in our case include the maximum current density, fall and rise times of the impulse waveform – see Section 5 for details), vector $\boldsymbol{\xi}$ denotes the parameters of the mechanical load, $F_{[0,T]}(\mathbf{g}, \boldsymbol{\theta}, \boldsymbol{\xi})$ is the design/performance fitness function of the structure that is observed during time interval $[0,T]$, constraints (9b) and (9c) represent the system of governing PDEs (8) with boundary conditions (7), respectively, and $\underline{\boldsymbol{\theta}}$ and $\overline{\boldsymbol{\theta}}$ are the lower and upper bounds for the vector of control variables $\boldsymbol{\theta}$. Note that for the sake of simplicity, we omit the explicit dependency of $\mathbf{g}$ on the time variable t.

As the purpose of our optimization problem is to minimize the post-impact vibrations of the plate, the optimization criterion F in (9) is defined as the average squared middle plane displacement of the plate:

$$F_{[0,T]}(\mathbf{g}, \boldsymbol{\theta}, \boldsymbol{\xi}) = \frac{1}{T} \int_0^T \left(w_c(\boldsymbol{\theta}, \boldsymbol{\xi}, t) \right)^2 dt, \tag{10}$$

where $w_c = w|_{y=0}$ is the middle plane displacement at the center of the plate.

3.2 A two-stage stochastic programming formulation

It can be readily seen that the optimal parameters of the electromagnetic field as a solution of problem (9) depend heavily on the parameters of the applied impact load. Since the impact load can rarely be predicted or estimated with sufficient accuracy, in this subsection we discuss a stochastic extension of the general problem (9) under the assumption that the impact load is uncertain, or random.

To deal with the uncertainty in the parameters of the impact load, we resort to the *two-stage stochastic optimization* framework. In general, the discipline of stochastic optimization is concerned with determining optimal decision policies in situations when the decision making process is influenced by uncertainties in problem data (Prékopa, 1995; Kall and Mayer, 2005; Shapiro et al, 2009; Birge and Louveaux, 2011). One of the main assumptions within this framework is that the uncertain parameters can be described probabilistically as random variables from some probability space $(\Omega, \mathscr{F}, \mathsf{P})$, where Ω is the set of random events, $\mathscr{F}$ is the sigma-algebra, and P is the probability measure. In other words, while the values of the uncertain parameters cannot be predicted with high degree of certainty, their probability distributions are believed to be known. The second assumption that is prevalent in most of stochastic optimization literature is that the probability distributions in question are *finite* ($|\Omega| < \infty$), and uncertainty in any given parameter ξ can be described by a finite set of possible realizations $\xi(\omega_1), \ldots, \xi(\omega_N)$, or *"scenarios"*, with each realiza-

tion (scenario) $\omega_i \in \Omega$ having a prescribed non-zero probability $\mathsf{P}(\omega_i) > 0$.

The two-stage stochastic optimization framework models the situation when the decision-making process under uncertainty involves two decisions, or actions: the initial, or *first stage* decision/action, and a subsequent corrective, or *recourse*, or *second stage* decision/action. Namely, the first-stage action is selected *under uncertainty,* i.e., before the actual realizations of the uncertain factors can be observed. After the first-stage decision has been made, it is assumed that one can observe the actual *realized* values of the problem's uncertain parameters as well as their effect on the outcome of that decision (e.g., a person must place a bet in a horse race before its start; then the outcome of the race and the bet determine the winnings, if any).

Clearly, in most cases the first-stage action will not be optimally suited for any given realization of uncertainty. The second-stage, or recourse decision/action is made *after* the particular realization of uncertainties was observed, and its purpose is to correct the consequences of the first-stage action with respect to the actual observed outcome of uncertainty. It is important to emphasize that the second-stage decision is dependent on the observed realization of uncertainties and the first-stage decision; in turn, the first-stage decision must take into account the probability distribution of uncertainties and the corresponding second-stage actions (for example, a poorly chosen first-stage action may not allow for any *feasible* corrective actions).

Mathematically, a two-stage stochastic optimization problem can be written in the form:

$$\begin{aligned} \min \quad & \mathsf{E}_\omega\big(f_1(\mathbf{x},\omega) + f_2(\mathbf{x},\mathbf{y}(\omega),\omega)\big) \\ \text{s. t.} \quad & \mathbf{h}_1(\mathbf{x},\omega) \le \mathbf{0}, \quad \forall \omega \in \Omega, \\ & \mathbf{h}_2(\mathbf{x},\mathbf{y}(\omega),\omega) \le \mathbf{0}, \quad \forall \omega \in \Omega. \end{aligned} \tag{11}$$

Here, $\mathbf{x}$ denotes the vector of first-stage decisions and $\mathbf{y} = \mathbf{y}(\omega)$ denotes second-stage decision; note that we explicitly indicate its dependence on the random element ω from the set Ω of all possible random events. Function $f_1(\mathbf{x},\omega)$ denotes the first-stage design/decision criterion, and $f_2(\mathbf{x},\mathbf{y}(\omega),\omega)$ denotes the corresponding criterion for the second-stage action. Similarly, $\mathbf{h}_1(\mathbf{x},\omega) \le \mathbf{0}$ represents the first-stage constraints to be satisfied by the first-stage decision $\mathbf{x}$, and the next constraint stipulates that the second-stage constraints to be satisfied by the second-stage decision $\mathbf{y}(\omega)$ may depend explicitly on first-stage decision $\mathbf{x}$ and the observed realization of ω. An optimal solution of (11) delivers the best, on average, value of the first- and second-stage design criteria.

With respect to the problem of impact of a composite plate that was discussed in Section 2.2, we consider that the vector $\boldsymbol{\xi}$ of parameters that describe the mechanical impact load $p_z(t) = p_z(t;\boldsymbol{\xi})$ is random, $\boldsymbol{\xi} = \boldsymbol{\xi}(\omega)$, with a known distribution. Probability space Ω is finite and describes a finite number of scenarios, $\Omega = \{\omega_1,\dots,\omega_N\}$, where each scenario ω_i corresponds to a specific vector of parameters $\boldsymbol{\xi}(\omega_i)$ of the impact load, and the probabilities $\mathsf{P}(\omega_i)$ of random elements $\omega_i \in \Omega$ are known. The discrete scenarios may represent, for example, different types of foreign objects that may strike the composite plate.

It is assumed that the actual realization of the parameters of impact load, $\hat{\boldsymbol{\xi}} = \boldsymbol{\xi}(\omega_k)$ for some $\omega_k \in \Omega$, becomes known (observable) after a certain time T_0 (for example, an appropriate sensor technology can be employed to estimate the impact load during the impact event). The decision on the choice of control parameters $\boldsymbol{\theta}$ must be made at or prior to $t = 0$, before the actual realization $\hat{\boldsymbol{\xi}}$ of the mechanical load can be observed. After time T_0, we have an opportunity for a corrective (recourse) action, which consists in adjusting the electromagnetic field so as to address the mismatch between the first-stage decision and the actual observation of uncertain parameters in the best way possible.

Specifically, during the first stage one applies an electromagnetic field with pre-computed parameters $\boldsymbol{\theta}$ so as to minimize the expected vibrations during the time period $t \in [0,T_0]$. It is assumed that during this time interval the profile of the mechanical load can be observed and identified, which allows for a subsequent correction $\boldsymbol{\theta}' = \boldsymbol{\theta}'(\omega)$ of the original selection $\boldsymbol{\theta}$, where we again explicitly indicate that the second-stage action $\boldsymbol{\theta}'$ depends on the observed realization $\omega \in \Omega$. Then, the two-stage stochastic PDE-constrained optimization problem that minimizes the plate's expected deflections can be formulated as:

$$\begin{aligned} \min_{\boldsymbol{\theta},\boldsymbol{\theta}'} \ & \mathsf{E}_\omega\Big(F_{[0,T_0]}\big(\mathbf{g}(\omega),\boldsymbol{\theta},\boldsymbol{\xi}(\omega)\big) \\ & \qquad + F_{[T_0,T_1]}\big(\mathbf{g}'(\omega),\boldsymbol{\theta}'(\omega),\boldsymbol{\xi}(\omega)\big)\Big) \end{aligned} \tag{12}$$

s. t.

$$\frac{\partial \mathbf{g}(\omega)}{\partial y} = \boldsymbol{\Phi}\left(\mathbf{g}, \frac{\partial \mathbf{g}}{\partial t}, \frac{\partial^2 \mathbf{g}}{\partial t^2}, \boldsymbol{\theta}, \boldsymbol{\xi}(\omega)\right), \ t \in [0,T_0], \ \forall \omega \in \Omega,$$

$$\mathbf{G}\left(\mathbf{g}(\omega), \frac{\partial \mathbf{g}(\omega)}{\partial t}\right)\Big|_{y=\pm\frac{a}{2}} = \mathbf{0}, \ t \in [0,T_0], \ \forall \omega \in \Omega,$$

$$\frac{\partial \mathbf{g}'(\omega)}{\partial y} = \boldsymbol{\Phi}\left(\mathbf{g}', \frac{\partial \mathbf{g}'}{\partial t}, \frac{\partial^2 \mathbf{g}'}{\partial t^2}, \boldsymbol{\theta}'(\omega), \boldsymbol{\xi}(\omega)\right), \quad t \in [T_0,T_1], \ \forall \omega \in \Omega,$$

$$\mathbf{G}\left(\mathbf{g}'(\omega), \frac{\partial \mathbf{g}'(\omega)}{\partial t}\right)\Big|_{y=\pm\frac{a}{2}} = \mathbf{0}, \ t \in [T_0,T_1], \ \forall \omega \in \Omega,$$

$$\mathbf{g}\big|_{t=T_0} = \mathbf{g}'\big|_{t=T_0}, \ \left.\frac{\partial \mathbf{g}}{\partial t}\right|_{t=T_0} = \left.\frac{\partial \mathbf{g}'}{\partial t}\right|_{t=T_0}, \ \forall \omega \in \Omega,$$

$$\underline{\boldsymbol{\theta}} \le \boldsymbol{\theta}, \boldsymbol{\theta}'(\omega) \le \overline{\boldsymbol{\theta}}, \quad \forall \omega \in \Omega.$$

Note the explicit dependence of vectors $\mathbf{g}(\omega)$, $\mathbf{g}'(\omega)$, $\boldsymbol{\theta}'(\omega)$, and $\boldsymbol{\xi}(\omega)$ on the random element $\omega \in \Omega$. The first term in the objective function of problem (12) corresponds to the first stage, when the parameters of the problem $\boldsymbol{\xi}(\omega)$

are uncertain with a known discrete distribution. During this stage, an electromagnetic field characterized by vector of parameters $\boldsymbol{\theta}$ is applied to minimize the expected value of $F_{[0,T_0]}\big(\mathbf{g}(\omega),\boldsymbol{\theta},\boldsymbol{\xi}(\omega)\big)$, the average squared middle plane displacement at the center of the plate during time interval $[0,T_0]$. The first two constraints in (12) stipulate that the governing PDEs (8) and boundary conditions (7) must hold at $t\in[0,T_0]$ for any of the possible impact load scenarios.

The second term in the objective of (12) represents the average squared middle plane displacement at the center of the plate during the second stage, from $t=T_0$ to $t=T_1$, which depends explicitly on the second-stage action $\boldsymbol{\theta}'(\omega)$ and implicitly on the preceding first stage action $\boldsymbol{\theta}$, by means of the continuity conditions that are given as the fifth line of constraints in (12). The values of vector $\mathbf{g}$ during time interval $[T_0,T_1]$ are denoted as $\mathbf{g}'$, and the third and fourth constraints of (12) require that the governing equations and boundary conditions hold during $[T_0,T_1]$ for all scenarios $\omega\in\Omega$. The fifth line of constraints (12) represents the continuity conditions at $t=T_0$ for the first-and second-stage mechanical fields $\mathbf{g}$ and $\mathbf{g}'$.

Since the space Ω is assumed to be finite, expectation in the objective function of problem (12) can be computed in the form of a finite sum (see Section 4.5). In situations when the stochastic parameters in the problem have continuous distributions, a satisfactory approximation of the expectation via a finite sum can be achieved by sampling an appropriate number of scenarios from that distribution. Typically, this requires a large number of samples (scenarios) and leads to large-scale stochastic optimization problems. A variety of different techniques have been developed in the literature to address the computational challenges associated with large-scale scenario sets in stochastic programming problems, which include methods that exploit the specific structure of the objective and constraints (various decomposition methods) as well as statistics-based methods (stochastic decomposition, sample average approximation, etc.), see Birge and Louveaux (2011). A detailed discussion of applicability of these techniques to formulation (12) is beyond the scope of this work; here we assume without loss of generality that the cardinality of space Ω is such that problem (12) is computationally tractable.

The two-stage stochastic PDE-constrained optimization problem (12) formalizes the proposed approach to control of mechanical structures under uncertainties with respect to the considered problem of impact of a composite plate. Clearly, the proposed framework allows for obvious generalizations with respect to the types of structures and applied mechanical loads, and, to a large degree, the type and mechanism of multifield coupling. Also, it is worth emphasizing that the PDE-constrained formulation (12) is a "true" two-stage stochastic optimization model, where both stages of control/action have physical meaning. This makes for an important difference with the work of Conti et al (2009), who formulated a topology optimization problem with uncertain loads in the two-stage form (11) by introducing an "artificial" second stage that consisted in solving the governing PDEs (physically, once a shape was selected, it could not be corrected or updated in response to the observed realization of stochastic load). Further, the governing PDEs in that work were assumed to be linear, which allowed the authors to propose a more efficient solution technique.

In the remainder of the paper we discuss the numerical solution procedures for problem (12) as well as physical viability of its solutions.

4 Numerical solution and optimization methods

In this section we discuss the basic steps of solution procedure for the two-stage stochastic PDE-constrained problem (12) in the case of an impacted composite plate as presented in Section 2.2.

4.1 Numerical solution of the governing system of PDEs

Presence of a system of nonlinear PDEs as constraints in problem (12) necessitates effective solution methods for the respective PDEs in order to solve (12). With respect to the specific boundary value problem for the plate subjected to impact and electromagnetic loads, we employ the methods proposed in Zhupanska and Sierakowski (2007); Barakati and Zhupanska (2012a). For the sake of completeness of the exposition, we outline the key points of the corresponding solution procedure below.

The system of nonlinear governing PDEs (8) that enters the two-stage PDE-constrained problem (12) can be rewritten in the form:

$$\frac{\partial\mathbf{g}}{\partial y}=\boldsymbol{\Phi}\left(\mathbf{g},\frac{\partial\mathbf{g}}{\partial t},\frac{\partial^2\mathbf{g}}{\partial t^2},y,t,\boldsymbol{\theta},\boldsymbol{\xi}\right), \tag{13}$$

where $\mathbf{g}=\mathbf{g}(x,y,t,\boldsymbol{\theta})$ is a vector of variables $\mathbf{g}=[v,w,W,N_{yy},N_{yz},M_{yy},E_x,B_z]$, $\boldsymbol{\Phi}$ is a nonlinear function from (8), and $\boldsymbol{\theta}$ is the optimization variable, i.e., the vector containing the parameters of the electromagnetic field (to be defined in Section 5).

A numerical solution procedure for this systems consists of a sequential application of a finite difference time integration, quasilinearization of the resulting system of the nonlinear ordinary differential equations (ODEs), and a finite difference spatial integration of the obtained two-point boundary value problem. The first step is to discretize (13) with respect to time t by applying Newmark finite difference time integration scheme (Newmark, 1959). This reduces (13) to

the nonlinear two-point boundary problem for the system of ODEs:

$$\frac{d\mathbf{g}}{dy} = \boldsymbol{\Phi}_1(\mathbf{g}, y, \boldsymbol{\theta}, \boldsymbol{\xi}), \tag{14}$$

This system is solved at discrete moments of time with timestep Δt by using a quasilinearization method of Bellman and Kalaba (1965). This method allows for substituting the solution of (14) with a sequential solution of a linearized system with linearized boundary conditions:

$$\begin{aligned}
&\frac{d}{dy}\mathbf{g}^{k+1} = \boldsymbol{\Phi}_1\left(\mathbf{g}^k, y, \boldsymbol{\theta}, \boldsymbol{\xi}\right) + \mathbf{A}\left(\mathbf{g}^k, y, \boldsymbol{\theta}, \boldsymbol{\xi}\right)\left(\mathbf{g}^{k+1} - \mathbf{g}^k\right),\\
&\left\{A_{ij}\left(\mathbf{g}^k, y, \boldsymbol{\theta}, \boldsymbol{\xi}\right)\right\} = \left\{\frac{\partial \Phi_{1_i}\left(\mathbf{g}^k, y, \boldsymbol{\theta}, \boldsymbol{\xi}\right)}{\partial g_j}\right\},\\
&\mathbf{D}_1\left(\mathbf{g}^k\right)\mathbf{g}^{k+1}\left(y_0\right) = \mathbf{d}_1\left(\mathbf{g}^k\right),\\
&\mathbf{D}_2\left(\mathbf{g}^k\right)\mathbf{g}^{k+1}\left(y_N\right) = \mathbf{d}_2\left(\mathbf{g}^k\right),
\end{aligned} \tag{15}$$

where $\mathbf{g}^{k+1}$ and $\mathbf{g}^k$ are the solutions at the current and previous iteration steps, respectively. A good choice for the initial guess $\mathbf{g}^0$ is a solution from the previous time step. Points y_0 and y_N correspond to the edges of the plate, matrices $\mathbf{D}_i\left(\mathbf{g}^k\right)$ and vectors $\mathbf{d}_i\left(\mathbf{g}^k\right)$, $i = 1,2$, are derived from the boundary conditions at $y = y_0$ and $y = y_N$. The sequence $\left\{\mathbf{g}^{k+1}\right\}$ of solutions of system (15) converges quickly to the solution of the nonlinear system and the stopping criterion for the iterative procedure is:

$$\max_i \left| g_i^{k+1}/g_i^k - 1 \right| \leq \delta, \tag{16}$$

where $\delta > 0$ is the prescribed accuracy.

To solve the system of linear ODEs in (15) we employ the superposition method (Atkinson et al, 2009). If M is the dimensionality of the system and there are $M/2$ boundary conditions on both the left ($y = y_0$) and right ($y = y_N$) ends, then we may represent the solution of the system of the linear ODEs by a linear combination of $M/2$ linearly independent general solutions of the homogeneous system and one particular solution of the inhomogeneous system:

$$\mathbf{g}^{k+1}(y) = \sum_{j=1}^{M/2} c_j \mathbf{G}^j(y) + \mathbf{G}^{\frac{M}{2}+1}(y), \tag{17}$$

where c_j are the linear coefficients. The values of $\mathbf{G}^j$, $j = 1, \ldots, \frac{M}{2}+1$ are obtained on the left end from the boundary conditions and then are propagated to the right end with the aid of the fourth-order Runge-Kutta method. At the right end the linear coefficients c_j can be found from the boundary conditions by solving a system of linear algebraic equations. In order to guarantee that vectors $\mathbf{G}^j$ are independent, and therefore coefficients c_j are uniquely determined at the right end, an orthonormalization procedure is employed after each iteration of the Runge-Kutta method. The corresponding transformation matrices are then used to restore the coefficients c_j.

4.2 PDE-constrained optimization framework

The existing approaches to PDE-constrained optimization problems can generally be categorized into two groups (Herzog and Kunisch, 2010). The first group of methods fits under the umbrella of "black box" optimization. This framework implies that one is able to obtain certain information about the objective function, which usually includes the value of the function for any given feasible point, its gradient and, perhaps, its higher order derivatives (depending on which optimization algorithm is employed) at that point. This information is then used to further direct the search for an optimal solution. It must be emphasized, however, that PDE constraints are embedded in the computation of the objective and its gradient and thus need to be satisfied at every step of the algorithm, which potentially makes this approach computationally expensive. For example, in the present work the value of the objective function is obtained by numerically solving a system of nonlinear PDEs using the procedure described in Section 4.1.

An alternative "discretize-then-optimize" approach consists in, first, discretizing the system of PDEs and replacing the PDE constraints in the problem with the resulting discretizations, often in the form of linear constraints. This generally leads to improved computational efficiency, as the system of governing PDEs is not required to be solved at every step. On the other hand, this method is not applicable to every type of PDE-constrained problem; for example, in our case the governing system of nonlinear PDEs cannot be solved by straightforward discretization.

The specifics of our particular problem dictates the use of black-box first-order optimization procedure, which can be summarized as follows: (i) compute the objective function by solving the governing system of PDEs numerically; (ii) compute first-order information, i.e., the gradient of the objective function at the current feasible point; (iii) apply a first-order optimization algorithm.

The value of objective function in (12) depends on the solution of a system of PDEs, which makes analytical computation of its gradient impractical. To this end, numerical differentiation techniques, such as complex differentiation (Squire and Trapp, 1998) or some version of automatic differentiation (Rall, 1986) can be employed.

4.3 Numerical differentiation

The proposed solution approach for two-stage stochastic PDE-constrained optimization problem (12) is based on first-order methods and requires computation of the gradient of the objective function at a given feasible point. Specifically, we are interested in the full derivatives of $F_{[0,T]}\left(\mathbf{g}(\omega), \boldsymbol{\theta}, \boldsymbol{\xi}(\omega)\right)$ with respect to $\boldsymbol{\theta}$ and $F_{[T_0,T_1]}\left(\mathbf{g}'(\omega), \boldsymbol{\theta}'(\omega), \boldsymbol{\xi}(\omega)\right)$ with respect to $\left[\boldsymbol{\theta}, \boldsymbol{\theta}'(\omega)\right]$. The

function F itself has a quite simple structure, however, $\mathbf{g}$ and $\mathbf{g}'$ are implicitly dependent on parameters $\boldsymbol{\theta}$ and/or $\boldsymbol{\theta}'(\omega)$, as they are coupled through the system of governing equations (8). Next in this subsection we will not distinguish between $\boldsymbol{\theta}$ and $\boldsymbol{\theta}'(\omega)$ and refer to them as a single vector of parameters $\boldsymbol{\theta}$ that is used as an input to the system of governing equations.

There exists a number of methods for numerically computing a derivative of a function, among which are finite-difference method, adjoint method, complex differentiation, automatic (algorithmic) differentiation. In our work, we use the method which is closely related to both complex and automatic differentiation.

The complex differentiation method (Squire and Trapp, 1998; Martins et al, 2003, 2001) is applicable in case of an analytic function of a real variable. Instead of taking a small step in the direction of the real axis, as is customary in finite difference methods, a small increment is considered in the direction of the imaginary axis:

$$f(x+is) = f(x) + isf'(x) - \frac{s^2}{2!}f''(x) - i\frac{s^3}{3!}f'''(x) + O(s^4).$$

If s is small enough, by computing $f(x+is)$ one can obtain approximations to the values of $f(x)$ and $f'(x)$:

$$f(x) = \operatorname{Re} f(x+is) + O(s^2),\ f'(x) = \frac{\operatorname{Im} f(x+is)}{s} + O(s^2).$$

As it can be readily seen, the complex differentiation method offers a significant improvement in accuracy comparing to the traditional finite-difference approach at a relatively low computational overhead, as there is no a subtraction cancelation error. In practice, it allows for fast and stable computation of derivatives at almost machine precision. However, in the multivariate case, $f = f(\mathbf{x})$, $\mathbf{x} \in \mathbb{R}^m$, one would have to evaluate $f(\mathbf{x} + is\mathbf{e}_k)$, where $\mathbf{e}_k$ is the k-th orthant in $\mathbb{R}^m$, for each $k = 1,\dots,m$, in order to compute the gradient of f at the point $\mathbf{x}$. This obviously increases significantly the computational effort for evaluation of the gradient of $f(\mathbf{x})$. Alternative methods for numerical differentiation of multivariate functions that are based on the the same principle employ various generalizations of complex numbers.

Existing generalizations of complex numbers rely on different definitions of the imaginary unit. One of such generalizations is represented by *dual numbers* (Kantor and Solodovnikov, 1989; Piponi, 2004) of the form $a + \eta b$, where η is the *dual unit*, $\eta \neq 0$, $\eta^2 = 0$. Similarly, *hyper-dual numbers* have the form $a = a_0 + \eta_1 a_1 + \dots + \eta_m a_m$ with m imaginary dual parts η_i such that $\eta_i \eta_j = 0$ for all i, j. The arithmetic operations with hyper-dual numbers are defined as follows:

$$\begin{aligned} a+b &= a_0 + b_0 + \eta_1(a_1+b_1) + \dots + \eta_m(a_m+b_m), \\ ab &= a_0b_0 + \eta_1(a_1b_0 + a_0b_1) + \dots + \eta_m(a_0b_m + a_mb_0), \end{aligned}$$

$$\begin{aligned} a/b = \big(a_0b_0 + \eta_1(a_1b_0 - a_0b_1) + \dots \\ + \eta_m(a_mb_0 - a_0b_m)\big)/b_0^2. \end{aligned} \tag{18}$$

Then, given a multivariate function $f(x_1,\dots,x_m)$, each of its m arguments can be represented as a hyper-dual number with m imaginary parts. More precisely, let variable x_i at a given point x_i^0 be represented by a hyper-dual number whose real part is equal to x_i^0 and all imaginary parts are set to zero, with the exception of the i-th imaginary part which is set to 1. It can be shown that upon application of the above hyper-dual arithmetic rules (18) for computation of the (hyper-dual) value of f, one obtains that the real part of the result is equal to $f(x_1^0,\dots,x_m^0)$, and the i-th imaginary part is equal to $(\partial f/\partial x_i)\big|_{\mathbf{x}=\mathbf{x}^0}$. As an illustration, consider

$$f(x_1,x_2) = \frac{(x_1+x_2)x_1}{x_2}.$$

To find $\frac{\partial}{\partial x_1} f\big(x_1^0,x_2^0\big)$ and $\frac{\partial}{\partial x_2} f(x_1^0,x_2^0)$, let $x_1 = x_1^0 + \eta_1 1 + \eta_2 0$ and $x_2 = x_2^0 + \eta_1 0 + \eta_2 1$. Then

$$\begin{aligned} f(x_1,y_1) &= \frac{x_1^0\left(x_1^0+x_2^0\right)}{x_2^0} + \eta_1\frac{2x_1^0+x_2^0}{x_2^0} - \eta_2\left(\frac{x_1^0}{x_2^0}\right)^2 \\ &= f(x_1^0,x_2^0) + \eta_1\frac{\partial}{\partial x_1}f(x_1^0,x_2^0) + \eta_2\frac{\partial}{\partial x_2}f(x_1^0,x_2^0). \end{aligned}$$

The described technique is, in fact, a forward mode of automatic differentiation (Rall, 1986), when derivative information is propagated forward with the computations according the the differentiation chain rule. There are different variations of this framework; more discussion of automatic differentiation with hyper-dual numbers can be found in Rall (1986); Piponi (2004); Fike and Alonso (2011).

In our case we need the full derivative of $F_{[0,T_0]}\big(\mathbf{g}(\boldsymbol{\theta}),\boldsymbol{\theta},\boldsymbol{\xi}\big)$ with respect to $\boldsymbol{\theta}$. The structure of F itself is quite simple and $\partial F/\partial\boldsymbol{\theta}$ can be found analytically. The biggest difficulty is to find the derivative of $\mathbf{g}$ with respect to $\boldsymbol{\theta}$. To this end, the governing system of equations (8) is solved numerically using hyper-dual numbers. The imaginary dual parts of all the input parameters except $\boldsymbol{\theta}$ are set to zero, while the i-th component of vector $\boldsymbol{\theta}$ has the form $\theta_i = \theta_i^0 + \eta_i$, where θ_i^0 is the corresponding numerical value of the input parameter. The imaginary dual parts of the resulting hyper-dual values of the components of vector $\mathbf{g}$ then represent the sought partial derivatives of $\mathbf{g}$.

4.4 Optimization methods

After the value and the gradient of the objective function in (12) are computed, an iteration of a first-order optimization algorithm is performed. In this study, we employed the active set method due to Hager and Zhang (2006).

The algorithm consists of the nonmonotone gradient projection scheme and regular unconstrained conjugate gradient method and switches between them under certain conditions. We will outline the ideas of both of these methods and how they are connected. More details on the active set algorithm including convergence analysis can be found in Hager and Zhang (2006, 2005).

Nonmonotone gradient projection algorithm (NGPA) can be applied to the so-called "box-constrained" optimization problems of the form:

$$\min_{\mathbf{x}} \{f(\mathbf{x}) : \mathbf{l} \leq \mathbf{x} \leq \mathbf{u}\}.$$

Let us denote the feasible set of this problem as $\Theta = \{\mathbf{x} \in \mathbb{R}^n : \mathbf{l} \leq \mathbf{x} \leq \mathbf{u}\}$, and define $P(\mathbf{x})$ as the projection of a point in $\mathbb{R}^n$ on Θ:

$$P(\mathbf{x}) = \arg\min_{\mathbf{y}\in\Theta} \|\mathbf{x}-\mathbf{y}\|.$$

If $\mathbf{x}_k \in \Theta$ is the current iterate, we compute $\mathbf{x}'_k = \mathbf{x}_k - \alpha_k \mathbf{q}_k$, where $\mathbf{q}_k$ is the gradient of the objective function f at $\mathbf{x}_k$ and α_k is the corresponding step length. The point $\mathbf{x}'_k$ can be infeasible, so its projection $P(\mathbf{x}'_k)$ on the feasible set is computed. By using a nonmonotone line search in the direction of the vector $\mathbf{d}_k = P(\mathbf{x}'_k) - \mathbf{x}_k$, a new iterate $\mathbf{x}_{k+1}$ is found.

For unconstrained optimization problems, a conjugate gradient method can be used. Its main principle is that every step is made in the direction of steepest descent which is corrected by previous direction multiplied by some β:

$$\mathbf{x}_{k+1} = \mathbf{x}_k + \delta_k \mathbf{d}_k, \quad \mathbf{d}_{k+1} = -\mathbf{q}_{k+1} + \bar{\beta}^N_k \mathbf{d}_k, \quad \mathbf{d}_0 = -\mathbf{q}_0,$$

where δ_i is the step length chosen by inexact line search. In our work, the following conjugate gradient method by Hager and Zhang (2005) is used:

$$\bar{\beta}^N_k = \max\{\beta^N_k, \eta_k\}, \;\; \beta^N_k = \frac{1}{\mathbf{d}_k^\top \mathbf{x}_k}\left(\mathbf{x}_k - 2\mathbf{d}_k \frac{\|\mathbf{x}_k\|^2}{\mathbf{d}_k^\top \mathbf{x}_k}\right)^\top \mathbf{q}_{k+1},$$

$$\eta_k = \frac{-1}{\|\mathbf{d}_k\| \min\{\eta, \|\mathbf{q}_k\|\}}.$$

The nonmonotone gradient projection algorithm is globally convergent and in theory can deal with box-constrained optimization quite well. However, in practice its speed of convergence can be slow near a local minimizer. At the same time, the conjugate gradient method often has superlinear convergence for unconstrained optimization problems. The active set algorithm takes advantage of both these methods by using NGPA to determine active constraints (faces of the feasible set Θ, containing current iterate $\mathbf{x}_k$). Then, the conjugate gradient method is used to optimize over that face.

4.5 Solution procedure

Now, knowing all the main components of the solution procedure, we can assemble them together to show how the problem is solved. Since the system of governing equations is solved numerically by discretization, we modify appropriately expression (10) of the optimization criterion. Namely, assuming that the discretization time step Δt is sufficiently small, the integral in (10) can be approximated by:

$$F_{[0,T]}(\mathbf{g},\boldsymbol{\theta},\boldsymbol{\xi}) \simeq \frac{1}{T/\Delta t}\sum_{k=1}^{T/\Delta t}\left(w_c(\boldsymbol{\theta},\boldsymbol{\xi},t_k)\right)^2, \tag{19}$$

where the values of w_c are taken at time instants $t_k = k\Delta t$. Note also that the constant factor Δt in the above summation can be disregarded in the optimization problem since it is present as a constant scaling factor in the objectives of optimization problems (9) and (12).

The system of governing equations is solved using hyper-dual arithmetic to obtain the derivative of w_c with respect to $\boldsymbol{\theta}$ for each time step t_k. Knowing all the derivatives $\frac{\partial w_c}{\partial \theta_i}$, an approximation of the derivatives $\frac{\partial}{\partial \theta_i} F_{[0,T]}(\mathbf{g},\boldsymbol{\theta},\boldsymbol{\xi})$ can be found using the standard chain rule in (19). Given that the distribution of stochastic factors $\boldsymbol{\xi} = \boldsymbol{\xi}(\omega)$ in the two-stage stochastic PDE-constrained optimization problem (12) is assumed to be discrete with a finite support, and therefore can be modeled by a finite scenario set $\Omega = \{\omega_1, \ldots, \omega_N\}$, where $\mathsf{P}(\omega_i) > 0$ and $\sum_{i=1}^N \mathsf{P}(\omega_i) = 1$, problem (12) can be presented in the following form

$$\min_{\boldsymbol{\theta},\boldsymbol{\theta}'(\omega_i)} \sum_{i=1}^N \mathsf{P}(\omega_i)\Big(F_{[0,T_0]}\Big(\mathbf{g}(\omega_i),\boldsymbol{\theta},\boldsymbol{\xi}(\omega_i)\Big) + F_{[T_0,T_1]}\Big(\mathbf{g}'(\omega_i),\boldsymbol{\theta}'(\omega_i),\boldsymbol{\xi}(\omega_i)\Big)\Big) \tag{20a}$$

s. t.

$$\frac{\partial \mathbf{g}(\omega_i)}{\partial y} = \boldsymbol{\Phi}\left(\mathbf{g}(\omega_i), \frac{\partial \mathbf{g}}{\partial t}, \frac{\partial^2 \mathbf{g}}{\partial t^2}, \boldsymbol{\theta}^{(1)}, \boldsymbol{\xi}(\omega_i)\right), \quad t \in [0,T_0], \;\; \forall i \in \{1,\ldots,N\}, \tag{20b}$$

$$\mathbf{G}\left(\mathbf{g}(\omega_i), \frac{\partial \mathbf{g}(\omega_i)}{\partial t}\right)\Big|_{y=\pm\frac{a}{2}} = \mathbf{0}, \quad t \in [0,T_0], \;\; \forall i \in \{1,\ldots,N\}, \tag{20c}$$

$$\frac{\partial \mathbf{g}'(\omega_i)}{\partial y} = \boldsymbol{\Phi}\left(\mathbf{g}'(\omega_i), \frac{\partial \mathbf{g}'}{\partial t}, \frac{\partial^2 \mathbf{g}'}{\partial t^2}, \boldsymbol{\theta}^{(2)}(\omega_i), \boldsymbol{\xi}(\omega_i)\right), \quad t \in [T_0,T_1], \;\; \forall i \in \{1,\ldots,N\}, \tag{20d}$$

$$\mathbf{G}\left(\mathbf{g}'(\omega_i), \frac{\partial \mathbf{g}'(\omega_i)}{\partial t}\right)\Big|_{y=\pm\frac{a}{2}} = \mathbf{0}, \quad t \in [T_0,T_1], \;\; \forall i \in \{1,\ldots,N\}, \tag{20e}$$

$$\mathbf{g}(\omega_i)\big|_{t=T_0} = \mathbf{g}'(\omega_i)\big|_{t=T_0}, \;\; \frac{\partial \mathbf{g}(\omega_i)}{\partial t}\Big|_{t=T_0} = \frac{\partial \mathbf{g}'(\omega_i)}{\partial t}\Big|_{t=T_0}, \quad \forall i \in \{1,\ldots,N\}, \tag{20f}$$

$$\underline{\boldsymbol{\theta}} \le \boldsymbol{\theta},\ \boldsymbol{\theta}'(\omega_i) \le \bar{\boldsymbol{\theta}}, \quad \forall i \in \{1,\dots,N\}.$$

To find the first group of summands of the objective (20a), $F_{[0,T_0]}\big(\mathbf{g}(\omega_i),\boldsymbol{\theta},\boldsymbol{\xi}(\omega_i)\big)$, and their partial derivatives w.r.t. $\boldsymbol{\theta}$, the boundary-value problem (20b)–(20c) is solved numerically for each $\omega_i \in \Omega$ using hyper-dual numbers. For the second group of components of the objective, $F_{[T_0,T_1]}\big(\mathbf{g}'(\omega_i),\boldsymbol{\theta}'(\omega_i),\boldsymbol{\xi}(\omega_i)\big)$, the boundary-value problem (20d)–(20e) must be solved and the continuity conditions (20f) must be satisfied. Note that $\mathbf{g}'$ implicitly depends on $\boldsymbol{\theta}$, and thus in the gradient of $\mathbf{g}'$ there are twice as many components as in the gradient of $\mathbf{g}$. In practice, to take into account this implicit dependence and continuity conditions in computing the value and gradient of $F_{[T_0,T_1]}\Big(\mathbf{g}'(\omega_i),\boldsymbol{\theta}'(\omega_i),\boldsymbol{\xi}(\omega_i)\Big)$, system (20b)–(20e) is solved for $t \in [0,T_1]$, using hyper-dual numbers for each $\omega_i \in \Omega$, with control parameters being switched from $\boldsymbol{\theta}$ to $\boldsymbol{\theta}'(\omega_i)$ at time T_0. Then, the value of F and its derivatives, are computed according to (19) with first $T_0/\Delta t$ terms being ignored.

In order to perform optimization step of the active set algorithm, two systems of PDEs (20b, 20d) with boundary conditions (20c, 20e) in the constraints are solved in hyper-dual numbers for each $\omega_i \in \Omega$ per above. This enables one to compute the value and gradient of objective function (20a). The outlined computational procedure was implemented in C++ programming language.

5 Numerical results

In this section we report optimization results for a single-layer, transversely isotropic (x-axis is the axis of material symmetry and y-z is the plane of isotropy) carbon fiber reinforced composite plate of width $a = 0.1524$ m and thickness $h = 0.0021$ m. Elastic properties of the composite plate are as follows: Young's modulus in the fiber direction is $E_1 = 102.97$ GPa, Young's modulus in the transverse direction is $E_2 = 7.55$ GPa, Poisson's ratios are $\nu_{21} = \nu_{13} = 0.3$, density of the composite is $\rho = 1594$ kg/m^3, electrical conductivity in the fiber direction is $\sigma_1 = 39000$ S/m and electrical permittivity in the fiber direction is $\varepsilon_1 = 2.5015 \times 10^{-10}$ F/m. The plate is subjected to a transverse impact load (4) at the initial time moment, $t = 0$. Simultaneously, an electromagnetic load is applied and consists of the time-dependent electric current applied in the fiber direction (5) and constant in-plane magnetic field applied in the direction perpendicular to the electric current (6) (see Figure 1). Application of the electromagnetic load is expected to mitigate the effects of the mechanical impact by maximally reducing the post-impact vibrations of the plate.

The (randomized) applied impact load $\mathbf{p}$ (4) has the following profile, where the maximum impact pressure p_0 and the impact duration τ_p are uncertain parameters, which is indicated by their dependence on a random event $\omega \in \Omega$:

$$p_x(y,t) = 0, \quad p_y(y,t) = 0, \tag{21}$$

$$p_z(y,t) = \begin{cases} -p_0(\omega)\sqrt{1-\left(\dfrac{y}{b}\right)^2}\sin\dfrac{\pi t}{\tau_p(\omega)}, \\ \qquad\qquad |y| \le b, \quad 0 \le t \le \tau_p(\omega), \\ 0, \qquad\qquad b < |y| \le \dfrac{a}{2}, \quad t > \tau_p(\omega). \end{cases}$$

Here $b = 0.1h$ is the width of the impact zone.

In such a way, the vector $\boldsymbol{\xi}(\omega)$ of uncertain parameters in the two-stage stochastic PDE-constrained optimization problem (12) contains p_0 and τ_p:

$$\boldsymbol{\xi}(\omega) = \big[p_0(\omega), \tau_p(\omega)\big].$$

It is assumed that the set Ω of random events contains three equiprobable elements, or scenarios:

$$\Omega = \{\omega_1,\omega_2,\omega_3\}, \quad \text{where} \quad \mathsf{P}(\omega_i) = 1/3,\ i = 1,2,3.$$

In the context of the conceptual application described in Section 1.1, this corresponds to the composite plate being hit at random by, e.g., three possible types of foreign objects or projectiles. Table 1 presents the numerical values of the possible realizations of the maximum impact pressure and impact duration of the impact load (21). The small size of the scenario set is chosen specifically for the illustrative purposes of our computational experiments; in practice, realistic descriptions of uncertainties require larger scenario sets.

Scenario, ω	Probability, $\mathsf{P}(\omega)$	$p_0(\omega)$, MPa	$\tau_p(\omega)$, ms
ω_1	1/3	0.75	8.0
ω_2	1/3	1.0	10.0
ω_3	1/3	2.0	12.0

Table 1 Scenario realizations of the maximum impact pressure p_0 and impact duration τ_p of the mechanical impact load (21).

The duration T_0 of the first stage was set at $T_0 = 10$ ms, which is equal to the average duration of impact in the considered scenarios. This reflects our assumptions that an appropriate sensory technology will allow for estimating the parameters of impact load during the impact event (see Sections 1.1 and 3.2). The total duration of computational time was set at $T_1 = 50$ ms. According to the two-stage stochastic framework described in Section 3.2, the electromagnetic field in the configuration prescribed by the first-stage solution is applied at $t = 0$. At $t = T_0$, the parameters of the electromagnetic field are changed as dictated by the second-stage solution; in such a way, the durations of the first and second stages are 10 ms and 40 ms, respectively.

The parameters of the magnetic field (6) applied to the plate are as follows:

$$B_x = 0, \quad B_y = B_y^* = 1.0\ \text{T}, \quad B_z = 0, \tag{22}$$

and the density $\mathbf{J}(t)$ of the time-dependent electric current (5) applied in the fiber direction is

$$J_x(t) = J_0 e^{-t/\tau_e} \sin\frac{\pi t}{\tau_s}, \quad J_y(t) = J_z(t) = 0, \tag{23}$$

where J_0, τ_e, and τ_s are the parameters determining the electric current waveform, i.e., the maximum current density, fall and rise times. The quantities J_0, τ_e, and τ_s constitute the vector $\boldsymbol{\theta}$ of decision variables, or control parameters:

$$\boldsymbol{\theta} = [J_0, \tau_e, \tau_s].$$

It is worth noting that the magnitude of magnetic field B_y is not formally included in the vector $\boldsymbol{\theta}$, and is fixed at the given value of 1 T in accordance to (22). This is due to our observation that when B_y was allowed to vary within a prescribed bounds (the so-called "box constraints") $0 \le B_y \le \overline{B}$, at optimality the decision variable B_y always assumed the maximum possible value, $B_y = \overline{B}$. Hence, for simplicity the value of B_y was fixed as in (22). The rest of the decision variables were box-constrained as follows:

$$|J_0| \le 10^8 \text{ A/m}^2, \quad 10^{-5} \text{ s} \le \tau_s, \tau_e \le 10^9 \text{ s}, \tag{24}$$

where the prescribed range of allowable current density values was chosen so as to eliminate Joule heating considerations (more precisely, to ensure that the thermal effects associated with application of electric current are negligible, see Barakati and Zhupanska (2012b) for an in-depth discussion of this issue). The box constraints on the fall and rise times τ_e and τ_s are selected in order to ensure realistic current profiles (as in the case of the lower bound) as well as to avoid numerical difficulties with convergence of the described above optimization procedures (as in the case of the upper bound).

During the optimization procedure, the initial values for both first and second stage solution vectors $\boldsymbol{\theta}$ and $\boldsymbol{\theta}'(\omega)$, $\omega \in \Omega$, were chosen as follows: $J_0 = 1.0 \times 10^6$ A/m^2, $\tau_s =$ 4.8 ms, $\tau_e = 4.8$ ms.

We would like to comment briefly on the choice of the initial solution in our problem. In general, problems (12), (20) are non-convex, whereby the choice of the initial solution point is crucial for reaching a local or global minimum. In the present work, the initial solution was selected using the physics-based considerations presented in our preliminary studies on this subject (Chernikov et al, 2015), where a deterministic problem of vibration mitigation in composite plates via application of an alternating (not pulsed) current was considered. Particularly, it was observed that although the objective (10) is indeed non-convex, its value is much more sensitive to the changes in the current frequency than current amplitude. Moreover, the objective function exhibited a sequence of local minima, which corresponded to current frequencies that are approximately equal to multiples

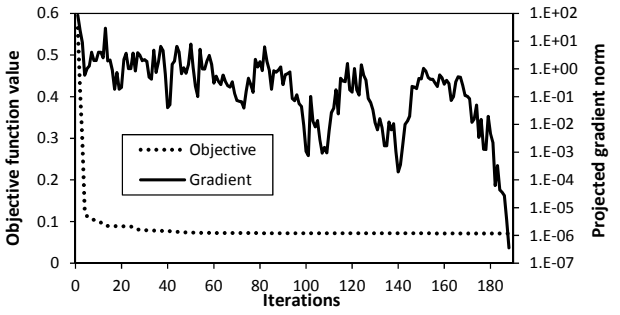

Fig. 2 Iteration history of the objective function value and the projected gradient norm

of the frequency of vibrations of the plate due to mechanical load only. To achieve the global minimum, the initial solution should have had current frequency close to the frequency of mechanical-only vibrations. These observations were taken into account when selecting the initial solution point as presented above.

Figure 2 illustrates the history of iterations of the values of the objective function (12) and the norm of its gradient during the optimization procedure described in Section 4.4.

The optimal solution of the two-stage stochastic PDE-constrained optimization problem (12) (or (20)) obtained during the described above solution process is presented in Table 2, which contains the parameters (J_0, τ_s, τ_e) of the waveform (23) of electric current as the components of the first-stage solution vector $\boldsymbol{\theta}$ and second-stage vectors $\boldsymbol{\theta}'(\omega_i)$, $i = 1,2,3$. The corresponding optimal waveform profiles of the electric current (23) are shown in Figure 3. Again, we emphasize the structure of the obtained two-stage stochastic solution: during the time interval $[0, T_0]$, i.e., from $t = 0$ until $t = 10$ ms, the optimal first-stage electric current ($J_0 = 2.51 \times 10^6$ A/m^2, $\tau_s = 11.12$ ms, $\tau_e = 19.65$ ms) is applied in order to minimize the expected plate deflection due to an uncertain impact load. According to the assumptions of our model, the parameters of the actual realization of the randomized impact load (i.e., the actual observed scenario) become known by time $t = T_0 = 10$ ms, and, depending on the observed scenario, the parameters of the electric current are "switched" at $t = T_0$ to the corresponding second-stage solution values so as to minimize post-impact vibrations of the plate. For example, if it is determined that the impact was "light", i.e., an impact load corresponding to scenario ω_1 was observed during $[0, T_0]$, then at $t = T_0$ the parameters of the electric current are changed to $J_0 = 10^8$ A/m^2, $\tau_s = 5.16$ ms, $\tau_e = 2.68$ ms.

The resulting vibrations of the plate during the time interval $[0, T_1]$ (i.e., from 0 to 50 ms) are displayed for each scenario, along with the corresponding current profile, in Figure 4. Note that in all three subfigures of Figure 4, the profile of the electric current between $t = 0$ and $t = 10$ ms

Table 2 Optimal parameters of the electric current (23) obtained after solving the two-stage stochastic PDE-constrained optimization problem (12).

Parameter	First stage	Second stage, scenario		
		ω_1	ω_2	ω_3
J_0, $10^6 \times$ A/m^2	2.51	100.0	1.02	100.0
τ_s, ms	11.12	5.16	9.07	3.71
τ_e, ms	19.65	2.68	0.01	3.08

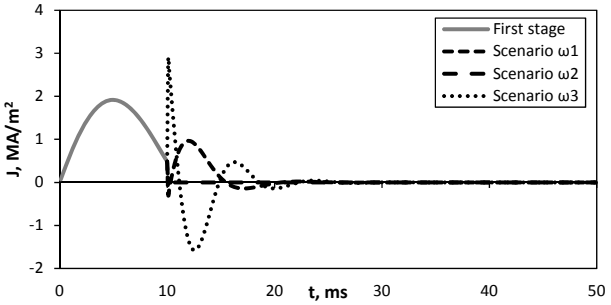

Fig. 3 Optimal electric current waveforms as specified in Table 2.

is the same and represents the first-stage solution (due to the differences in the maximum impact pressure across the scenarios, the subfigures use different scales on the vertical axes). It is also of interest to note that in scenarios ω_1 and ω_2 the electromagnetic load applied during the first stage is such that it causes the plate to deflect in the direction opposite to the direction of impact. This observation is also in accord with the formulated model: the first stage solution minimizes the plate deflection "on average"; in addition, the magnitude of maximum impact pressure in scenario ω_3 is two to almost three times higher than those in scenarios ω_1 and ω_2.

Figure 5 presents, for each of the three scenarios, the comparisons of the plate's transverse deflection with and without application of the (optimal) electromagnetic field. It is clear that the constructed two-stage stochastic optimization solution allows for significant suppression of vibrations caused by uncertain impact load in all three scenarios. It can be seen from Figure 5 that, while the developed two-stage model and the corresponding optimal parameters of the electromagnetic field result in substantial dampening of post-impact vibrations, the vibrations are not suppressed completely. This is a natural consequence of the fact that the impact load is uncertain, and therefore it is impossible to provide the "best" response to each of the possible scenarios.

Next we illustrate the effectiveness of the developed framework in the situation when the impact load is known beforehand, i.e., when it can be regarded deterministic. One can expect that in this case the parameters of the electromagnetic field can be tuned to achieve a much better mitigation of post-impact effects comparing to the stochastic case.

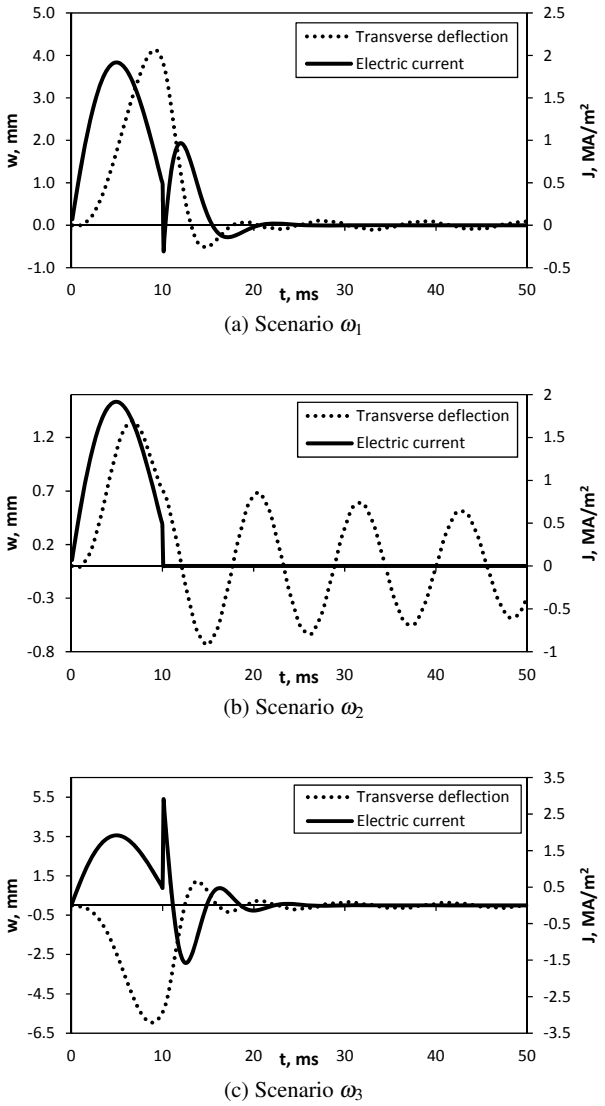

(a) Scenario ω_1

(b) Scenario ω_2

(c) Scenario ω_3

Fig. 4 Transverse deflection of the plate and optimal electric current waveforms corresponding to different impact load scenarios.

In particular, we assume that the deterministic impact load has the same parameters as the load of scenario ω_2, in accordance to expression (21) and Table 1. It is then convenient to consider that the stochastic problem is solved under the assumption that all scenarios, except ω_2, are impossible, i.e.,

$$\mathsf{P}(\omega_1) = 0, \quad \mathsf{P}(\omega_2) = 1, \quad \mathsf{P}(\omega_3) = 0.$$

This implies that in the scenario-based formulation (20) of the two-stage stochastic PDE-constrained optimization problem (12) the terms in the objective function that correspond to scenarios ω_1 and ω_3 are eliminated, and, in addition, the constraints that enforce satisfaction of the PDE

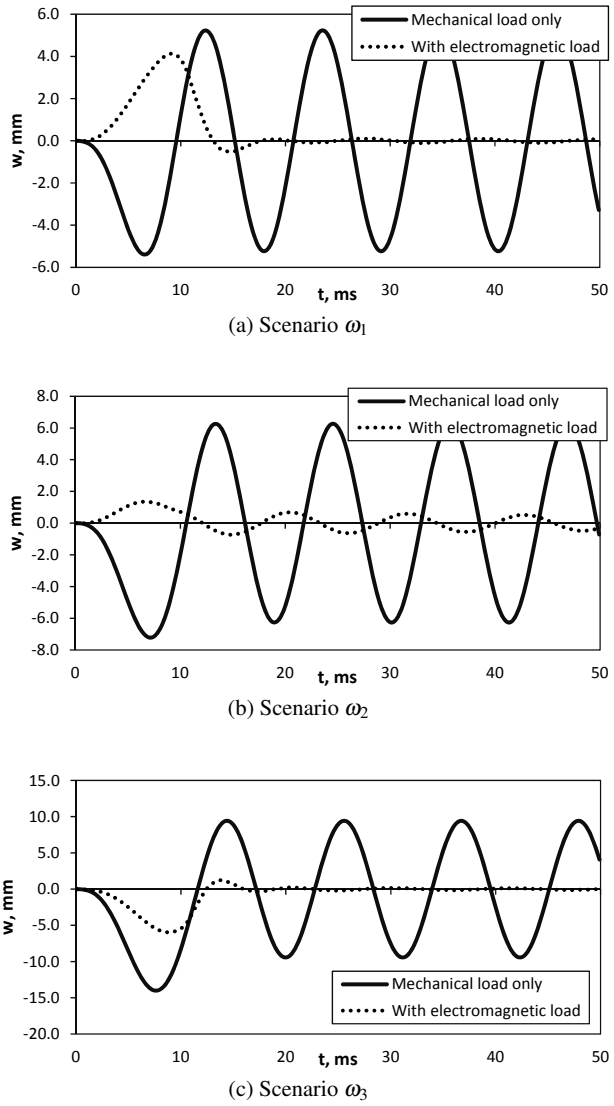

(a) Scenario ω_1

(b) Scenario ω_2

(c) Scenario ω_3

Fig. 5 Transverse deflection in the center of the plate vs. time for different scenarios.

equations and boundary conditions in scenarios ω_1, ω_3 are also disregarded.

Note, however, that the two-stage structure of the solution of (20) is still preserved, which means that at $t = T_0$ the parameters of the applied electric current are allowed to change. In other words, electric currents of two different waveforms determined by $\boldsymbol{\theta}$ and $\boldsymbol{\theta}'(\omega_2)$ are applied during time intervals $[0, T_0]$ and $[T_0, T_1]$, respectively. During the time interval $[0, T_0]$, electric current with parameters given by the first stage solution $\boldsymbol{\theta}$ is used to optimally mitigate the impact itself, while during $[T_0, T_1]$ the electric current with parameters $\boldsymbol{\theta}'(\omega_2)$ then suppresses the post-impact effects.

With exception of modifications just described, the rest of the parameters of the problem are the same as before. The obtained solution of this deterministic problem is given in Table 3. Figure 6 shows the transverse middle plane deflection, w_c, at the center of the plate, $y = 0$, as a function of time for the cases when only the mechanical load is present, and when the optimal electromagnetic field is applied as well. It is easy to see that in a deterministic setting the proposed framework is capable of practically eliminating the vibrations.

Table 3 Optimal parameters of the electric current in the deterministic case when impact load has the same parameters as in scenario ω_2 of the stochastic case.

Parameter	First stage	Second stage, ω_2
J_0, $10^6 \times$ A/m^2	1.69	4.78
τ_s, ms	10.01	5.82
τ_e, ms	133.21	1.89

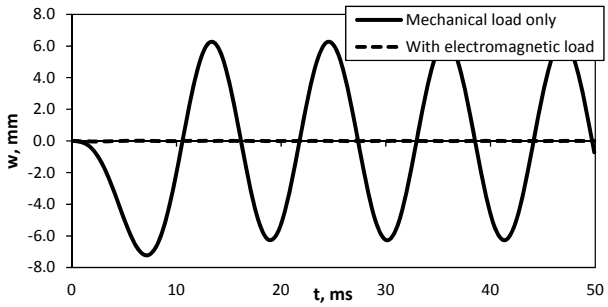

Fig. 6 Transverse deflection of the plate in the deterministic case that is based on scenario ω_2.

6 Conclusions

In this work, a two-stage stochastic PDE-constrained optimization methodology is developed for the active vibration control of structures in the presence of uncertainties in mechanical loads. The solution methodology includes a black-box first-order optimization procedure embedded in the two-stage stochastic optimization formulation. The black-box first-order optimization procedure consists of solving a system of governing PDEs and automatic differentiation with hyper-dual numbers for computing the objective function and its gradient, respectively; and applying a first-order active-set algorithm with a conjugate gradient method for solving the optimization problem.

The developed optimization methodology is applied to the problem of post-impact vibration control (via applied electromagnetic filed) of an electrically conductive carbon fiber reinforced composite plate subjected to a stochastic impact load. The system of governing PDEs describing such a problem consists of nonlinear equations of motion and Maxwell's equations. The randomized impact load applied to the plate is modeled by equiprobable scenarios with different parameters of maximum impact pressure and impact

duration. The electromagnetic load is comprised of a time-dependent electric current applied in the fiber direction and a constant in-plane magnetic field applied in the direction perpendicular to the electric current. Electric current waveform characteristics (i.e., the maximum current density, fall and rise times) constitute the vector of optimization variables, or control parameters. The optimal solution of the two-stage stochastic PDE-constrained optimization problem represents a sequence of control actions, where the first-stage electric current waveform is applied at the moment of impact without knowing the actual impact load parameters; the second-stage electric current waveform represents a corrective action, which is applied when the parameters of the actual impact load have been observed/identified. The results show that the constructed two-stage optimization solution allows for a significant suppression of vibrations caused by the randomized impact load in all impact load scenarios. Lastly, the effectiveness of the developed methodology is illustrated in the case of a deterministic impact load, where the two-stage strategy enables one to practically eliminate post-impact vibrations.

The two-stage stochastic control framework is applicable to many engineering problems involving physical systems that are subject to uncertain conditions. The developed two-stage stochastic PDE-constrained optimization formulation can generally be extended to mechanical engineering problems where field coupling effects can be used to change the mechanical response of solids, fluids, and structures. In particular, possible extensions include stochastic control of piezomaterials, magnetorheological fluids, etc.

Acknowledgements Olesya Zhupanska and Dmitry Chernikov would like to acknowledge the support of DARPA, N66001-11-1-4133 (Disclaimer: Any opinions, findings, and conclusions or recommendations expressed in this publication are those of the authors and do not necessarily reflect the views of DARPA). Dmitry Chernikov is grateful for the support from the AFRL Mathematical Modeling and Optimization Institute during Summer 2013 and Summer 2014. Pavlo Krokhmal would like to acknowledge AFOSR grant FA9550-12-1-0142 and the U.S. Dept of Air Force grant FA8651-12-2-0010.

References

Atkinson KE, Han W, Stewart DE (2009) Numerical Solutions of Ordinary Differential Equations. John Wiley and Sons, Inc., New Jersey

Barakati A, Zhupanska OI (2012a) Analysis of the effects of a pulsed electromagnetic field on the dynamic response of electrically conductive composites. Applied Mathematical Modelling 36:6072–6089

Barakati A, Zhupanska OI (2012b) Thermal and mechanical response of a carbon fiber reinforced composite to a transverse impact and in-plane pulsed electromagnetic loads. Journal of Engineering Materials and Technology 134(3):031,004

Barakati A, Zhupanska OI (2013) Influence of the electric current waveform on the dynamic response of the electrified composites. International Journal of Mechanics and Materials in Design 9(1):11–20

Barakati A, Zhupanska OI (2014) Mechanical response of electrically conductive laminated composite plates in the presence of an electromagnetic field. Composite Structures 113:298–307

Bellman RE, Kalaba RE (1965) Modern Analytic and Computational Methods in Science and Mathematics. American Elsevier Publishing Company, Inc., New York

Birge JR, Louveaux F (2011) Introduction to Stochastic Programming, 2nd edn. Springer, New York

Chernikov D, Krokhmal P, Zhupanska OI (2015) Vibration mitigation in composite plates using an electromagnetic field. In: Proceedings of the 56th AIAA/ASCE/AHS/ASC Structures, Structural Dynamics & Materials Conference, Kissimmee, FL, p to appear

Conti S, Held H, Pach M, Rumpf M, Schultz R (2009) Shape optimization under uncertainty—a stochastic programming perspective. SIAM J on Optimization 19(4):1610–1632

Eringen AC (1989) Theory of electromagnetic elastic plates. International Journal of Engineering Science 27:363–375

Fike JA, Alonso JJ (2011) The development of hyper-dual numbers for exact second-derivative calculations. In: 49th AIAA Aerospace Sciences Meeting, vol 886

Gibson R (2010) A review of recent research on mechanics of multifunctional composite materials and structures. Composite Structures 92(12):2793–2810

Hager WW, Zhang H (2005) A new conjugate gradient method with guaranteed descent and an efficient line search. SIAM Journal on Optimization 16(1):170–192

Hager WW, Zhang H (2006) A new active set algorithm for box constrained optimization. SIAM Journal on Optimization 17(2):526–557

Hasanyan D, Librescu L, Ambur D (2006) Buckling and postbuckling of magnetoelastic flat plates carrying an electric current. International Journal of Solids and Structures 43:4971–4996

Hasanyan DJ, Piliposyan GT (2001) Modelling and stability of magnetosoft ferromagnetic plates in a magnetic field. Proceedings of the Royal Society A 457:2063–2077

Herzog R, Kunisch K (2010) Algorithms for pde-constrained optimization. GAMM-Mitteilungen 33(2):163–176

Higuchi M, Kawamura R, Tanigawa Y (2007) Magneto-thermo-elastic stresses induced by a transient magnetic field in a conducting solid circular cylinder. International Journal of Solids and Structures 44:5316–5335

Kall P, Mayer J (2005) Stochastic Linear Programming: Models, Theory, and Computation. Springer

Kang BS, Choi WS, Park GJ (2001) Structural optimization under equivalent static loads transformed from dynamic loads based on displacement. Computers & Structures 79(2):145–154

Kantor IL, Solodovnikov AS (1989) Hypercomplex Numbers: An Elementary Introduction to Algebras. Springer-Verlag, New York

Martins JRRA, Sturdza P, Alonso JJ (2001) The connection between the complex-step derivative approximation and algorithmic differentiation. In: 39th Aerospace Sciences Meeting and Exhibit, vol 921, p 2001

Martins JRRA, Sturdza P, Alonso JJ (2003) The complex-step derivative approximation. ACM Trans Math Softw 29(3):245–262

Maugin GA (1988) Continuum Mechanics of Electromagnetic Solids. North-Holland, Amsterdam

Min S, Kikuchi N, Park YC, Kim S, Chang S (1999) Optimal topology design of structures under dynamic loads. Structural optimization 17(2–3):208–218

Moon FC (1984) Magnetosolid Mechanics. Wiley, New York

Newmark NM (1959) A method of computation for structural dynamics. Journal of the Engineering Mechanics Division Proceedings of the ASCE 85:67–97

Piponi D (2004) Automatic differentiation, c++ templates, and photogrammetry. Journal of Graphics Tools 9(4):41–55

Prékopa A (1995) Stochastic Programming. Kluwer Academic Publishers

Rall LB (1986) The arithmetic of differentiation. Mathematics Magazine 59(5):pp. 275–282

Rudnicki M (2002) Eigenvalue solutions for free motion of electroconductive plate in magnetic field. International Journal of Engineering Science 40:93–107

Shapiro A, Dentcheva D, Ruszczyński A (2009) Lectures on Stochastic Programming: Modeling and Theory. SIAM, Philadelphia, PA

Squire W, Trapp G (1998) Using complex variables to estimate derivatives of real functions. SIAM Review 40(1):110–112

Zhang X, Kang Z (2014) Dynamic topology optimization of piezoelectric structures with active control for reducing transient response. Computer Methods in Applied Mechanics and Engineering 281(0):200–219

Zhupanska OI, Sierakowski RL (2007) Effects of an electromagnetic field on the mechanical response of composites. Journal of Composite Materials 41(5):633–652

Zhupanska OI, Sierakowski RL (2011) Electro-thermo-mechanical coupling in carbon fiber polymer matrix composites. Acta Mechanica 218(3–4):219–232